Bulletin of Earthquake Engineering
https://doi.org/10.1007/s10518-019-00656-7

ORIGINAL RESEARCH

Predictive model for seismic vulnerability assessment of churches based on the 2009 L'Aquila earthquake

Gianfranco De Matteis[1] · **Giuseppe Brando**[2] · **Valentina Corlito**[1]

Received: 29 December 2018 / Accepted: 28 May 2019

Abstract
Seismic events that struck Italy in the last years had a dramatic impact on historical and cultural heritage. Damage occurred on existing masonry buildings, in particular on churches, stressed out the need to better understand the seismic behaviour of this type of constructions as well as to define more appropriate mitigation strategies to be applied at large scale. This study deals with a predictive methodology for vulnerability assessment of churches in large territorial areas. Focusing the attention on three naves churches of Abruzzi, the paper proposes modifications and integrations of an existing methodology taken by literature. These modifications are defined through a calibration procedure based on damage observation of 64 three naves churches located at different distances from the epicentre of the 2009 earthquake. The proposed model is employed to predict damage level distribution for different earthquake intensities, allowing fragility curves to be plotted and therefore potential damage scenarios to be represented.

Keywords Predictive models · Fragility curves · Vulnerability assessment · L'Aquila earthquake · Masonry churches

1 Introduction

Masonry churches represent one of the most important assets of Italian cultural heritage. Their architectural, historical and social value strictly relates these constructions to the intrinsic identity of the related territory.

The earthquakes occurred in Italy in the last decades (i.e. Umbria e Marche earthquake 1997; L'Aquila earthquake 2009; Emilia Romagna earthquake 2012; Central Italy earthquake 2016) evidenced severe states of damage and, in the worst cases, significant losses of important churches, emphasising the fragility of these constructions. Typical examples are the churches of St. Gregorio in S. Gregorio (Aq), St. Paolo in Mirabello (Fe) and St. Maria in Argentea in Norcia (Pg), which undergone extensive collapses due to the earthquakes of

✉ Gianfranco De Matteis
gianfranco.dematteis@unicampania.it

[1] Department of Architecture and Industrial Design, University of Campania "Luigi Vanvitelli", Via San Lorenzo, Abazia di San Lorenzo, 81031 Aversa, CE, Italy

[2] Department of Engineering and Geology, University "G. d'Annunzio, Pescara, Italy

Published online: 01 June 2019

L'Aquila (2009, Mw 6.3), Emilia Romagna (2012, Mw 5.9) and Italia Centrale (2016, Mw 6.0–6.5) respectively, as shown in Fig. 1a–c. On the other hand, the church of Purgatorio in Casamicciola Terme (Na), damaged during the 2017 Ischia earthquake (Mw 3.9), shown in Fig. 1d, highlighted that Italian churches and masonry buildings could be affected by significant damage also in case of earthquakes of limited magnitude for certain specific features of the dynamic excitation (Del Gaudio et al. 2018).

All the above remarks underline that a better knowledge of the structural behaviour and of the seismic vulnerability of the churches, at different observational scale (D'Ayala 2000; Criber et al. 2015; Brando et al. 2015; Betti et al. 2018; Valente and Milani 2018), is of paramount importance to prevent losses through the definition of reliable preventive protection strategies (De Matteis et al. 2019a).

In particular, observational analyses at territorial scale carried out on churches in the aftermath of significant seismic events, such as Friuli (Doglioni et al. 1994), Umbria and Marche (Lagomarsino and Podestà 2004a, b), Molise (Lagomarsino and Podestà 2004c), L'Aquila (Lagomarsino 2012; Tashkov et al. 2010; De Matteis et al. 2019b) and Central Italy (Hofer et al. 2018; De Matteis and Zizi 2019) earthquakes, allowed to learn more about the most recurrent damage mechanisms, as well as the most influential sources of seismic fragility of churches. Different methodologies have been developed, considering various approaches for the collection and interpretation of data (Da Porto et al. 2012;

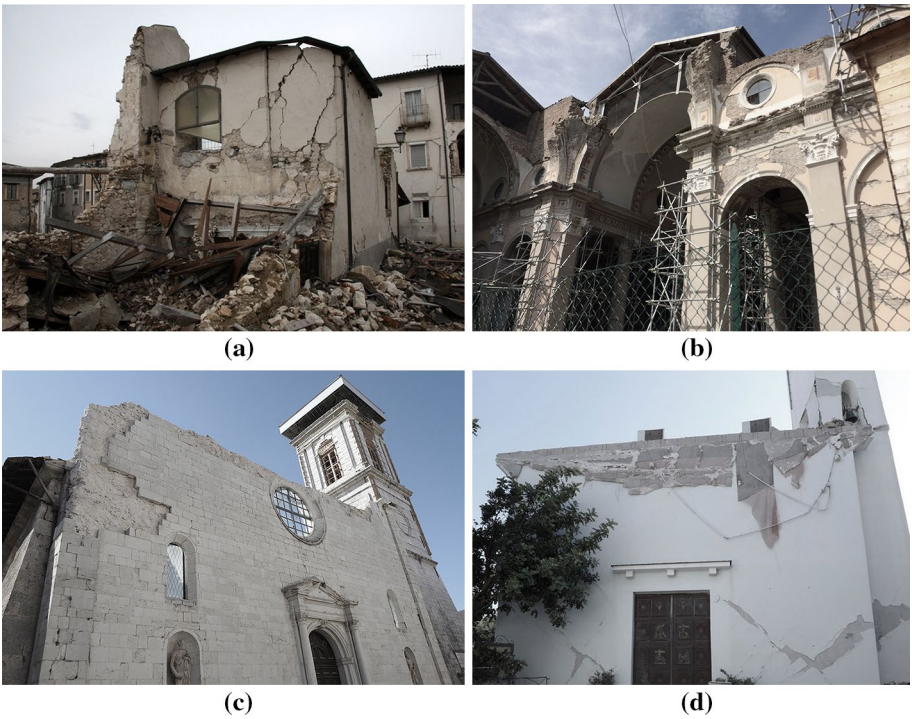

Fig. 1 State of damage observed in the Italian churches of St. Gregorio in S. Gregorio (AQ) (**a**), St. Paolo in Mirabello (FE) (**b**), St. Maria in Argentea in Norcia (PG) (**c**), and Purgatorio in Casamicciola (Na) (**d**) after the earthquakes of L'Aquila (2009, Mw 6.3), Emilia Romagna (2012, Mw 5.9), Italia Centrale (2016, Mw 6.0–6.5) and Ischia (2017, Mw 3.9), respectively

Marotta et al. 2016). The main outcomes mainly consisted in damage scenarios provided in terms of damage probability matrixes or fragility curves.

Alternative methodologies were also developed on the basis of analytical evaluations, mainly based on the study of macro-elements behaviour through linear and non-linear kinematic analyses (De Matteis and Mazzolani 2010). With general reference to the approach to be used for existing masonry buildings, the studies of Faccioli et al. (1999), Lang and Bachmann (2004), D'Ayala (2005), Milani and Lourenco (2011) and Brandonisio et al. (2013) are definitely worth of being mentioned.

Considering the evidences observed during further surveys carried out on new populations of churches damaged by more recent earthquakes, it is evident that the existing methodologies need to be refined and updated. Therefore, this paper aims at providing a predictive methodology for the vulnerability assessment of churches, which has been calibrated in the light of the observations carried out on a stock of 64 three naves churches hit by the 2009 L'Aquila earthquake.

The method is a modification of a procedure of the existing literature, which is currently adopted by the Italian Guidelines for Cultural Heritage (2011). It is based on the same shape of the vulnerability function proposed by Sandi and Floricel (1994), which was also used by other researchers (Giovinazzi and Lagomarsino 2004).

In this study, new coefficients for this function are proposed based on the outcomes of the damage observation of churches belonging to the dioceses of Sulmona-Valva and L'Aquila, in Abruzzi. The new formulation, which, differently by the previous studies in the literature, is focused on churches related to a specific territorial area (namely the Abruzzi region) and characterized by a three naves configuration, provides less conservative fragility curves with respect to the ones obtained from the aforementioned studies.

2 The investigated churches

2.1 General information

A large survey of old masonry churches belonging to both Sulmona-Valva [SU-VA] and L'Aquila [AQ] dioceses was carried out after the 2009 earthquake. The analysed territory is located in the hinterland of the Abruzzi region -in the Centre of Italy- and covers almost half of L'Aquila district. In this area, 77 municipalities were identified, with a total number of 635 old masonry churches.

The conducted observational survey was particularly focused on three naves churches, because they represent the most interesting and complex typology among those observed in Abruzzi. The above-mentioned stock of buildings was deeply analysed in a previous study (De Matteis et al. 2016), where a critical description of the whole stock of analysed churches was presented in terms of historical stratifications, architectural features and geometric issues.

In this paper, more attention is given to the structural and architectural features of these churches, which are directly employed for the application of the proposed vulnerability assessment procedure.

In Fig. 2, the analysed stock of churches is overlapped to the 2009 earthquake macroseismic intensity map (MCS scale). Totally, 64 three naves churches were observed. 26 churches (41% of the stock) belong to Sulmona-Valva diocese [SU-VA] and 38 churches to the L'Aquila diocese [AQ] (Fig. 3a). In Fig. 3b, the state of maintenance of the considered

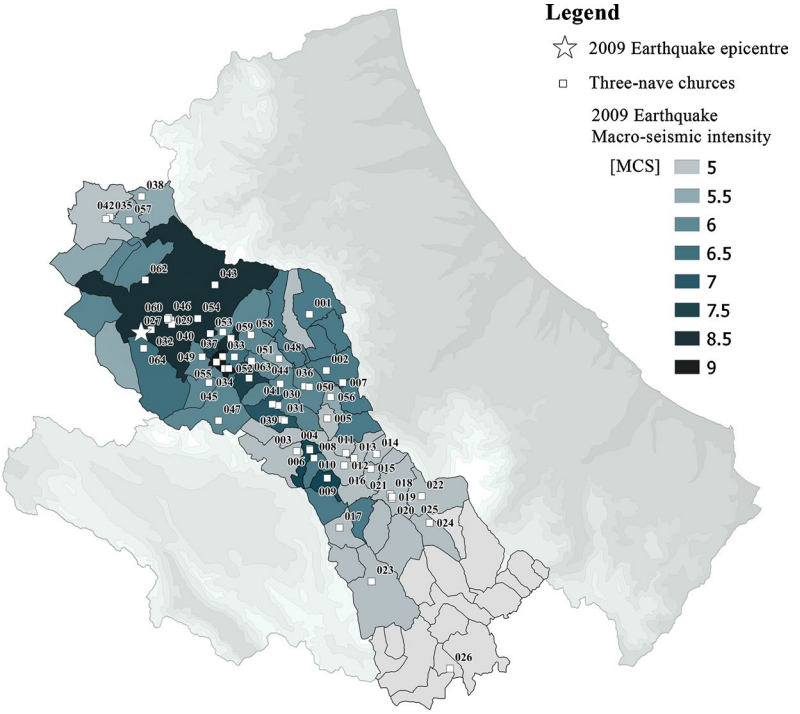

001	**SME**	San Marco Evangelista	023	**SMV**	Santa Maria delle Valle	045	**MPF**	Chiesa di S.Maria e S.Pietro
002	**SMP**	Santa Maria della Pace	024	**SSL**	San Salvatore	046	**SGT**	Chiesa di San Giovanni Battista
003	**SMA**	San Martino	025	**SNB**	San Nicola di Bari	047	**SAS**	Chiesa di Santa Maria Assunta
004	**SFR**	San Francesco	026	**SMC**	Santa Maria del Carmelo	048	**SPS**	Chiesa di Santa Maria in Pant.
005	**SBA**	San Benedetto Abate	027	**SBR**	Chiesa di San Bernardino	049	**SSB**	Chiesa di San Sebastiano
006	**SGE**	San Giovanni Batt ed Ev.	028	**SBM**	Chiesa di San Biagio d'Amit.	050	**SMU**	Chiesa di Santa Maria in Cer.
007	**SPO**	San Pietro ad Oratorium	029	**SDM**	Chiesa di San Domenico	051	**SPF**	Chiesa di San Panfilo d'Ocre
008	**SMS**	Santa Maria Assunta	030	**CLM**	Basilica di S.Maria di Collem.	052	**SFM**	Chiesa di San Felice Martire
009	**SGM**	Santa Gemma	031	**SMG**	Chiesa dei Ss. Mass. e Giorgio	053	**SNC**	Chiesa di San Nicandro
010	**SMN**	Santa Maria Nova	032	**SSV**	Chiesa di San Silvestro	054	**SLU**	Chiesa di Santa Lucia
011	**SMB**	Santa Maria del Borgo	033	**SBB**	Chiesa di San Benedetto Abate	055	**SPI**	Chiesa di San Pietro
012	**SMM**	Santa Maria Maggiore	034	**SAN**	Chiesa di Santa Maria Assunta	056	**SDE**	Chiesa di San Demetrio
013	**SPE**	San Pelino	035	**SGI**	Chiesa di San Giustino	057	**SPT**	Chiesa di San Pietro Celestino
014	**SMI**	San Michele Arcangelo	036	**SNM**	Chiesa dei Ss. Nican. e Marc.	058	**SEU**	Chiesa di Sant'Eusanio Martire
015	**MDL**	Madonna della Libera	037	**SGO**	Chiesa di San Gregorio Magno	059	**SGV**	Chiesa di San Giovanni Evang.
016	**SPC**	San Pietro Celestino	038	**SLB**	Chiesa di San Lorenzo	060	**SGG**	Santi Giusta e Giorgio
017	**SGR**	Santa Maria delle Grazie	039	**SFB**	Chiesa di San Flaviano	061	**SRO**	Chiesa di Santa Maria della R.
018	**SSA**	Santissima Annunziata	040	**SMX**	Chiesa di S. Maria di Pic. E.M.	062	**SPN**	Chiesa di Santa Maria del Ponte
019	**SPA**	San Panfilo	041	**SLO**	Chiesa di Santa Maria del Loreto	063	**SAR**	Chiesa di San Michele Arcang.
020	**SDO**	San Domenico	042	**SFC**	Chiesa di San Flaviano	064	**SAG**	Chiesa di Sant'Agata
021	**SMT**	Santa Maria della Tomba	043	**SSS**	Chiesa di Santa Maria Assunta			
022	**SMR**	Santa Maria Maggiore	044	**SGL**	Chiesa di San Giovanni Battista			

Fig. 2 The three naves churches in L'Aquila and Sulmona-Valva dioceses: location related to the 2009 earthquake macro-seismic intensity map (MCS scale)

population of churches is shown. Only a low percentage of them is currently in good condition (11%), whereas the remaining part is characterized by a poor conservation state due to absence of maintenance and presence of degraded elements, as can be for example observed in St. Salvatore church in Cansano [SSL; SU-VA] (Fig. 4).

In relation to their typology, the studied churches are characterized by different uses (Fig. 5a) with a clear prominence of parishes (the 62% of the stock); such an information stresses that a large part of the religious buildings is characterized by a high exposition

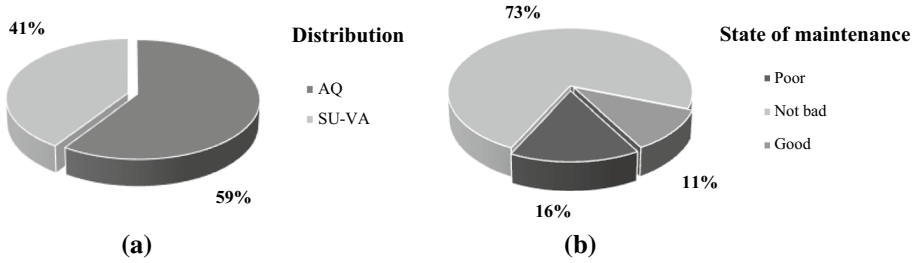

Fig. 3 Geographical distribution of investigated churches (**a**); state of maintenance (**b**)

Fig. 4 Degraded elements observed in St. Salvatore church in Cansano [SU-VA]

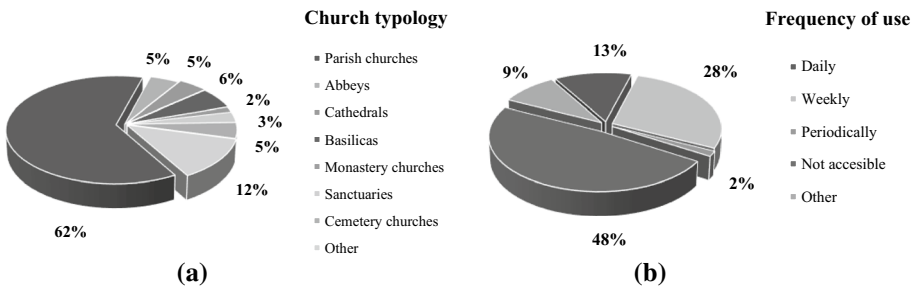

Fig. 5 Typology **a** and frequency of use **b** of investigated churches

of people at risk. In fact, among these churches, a wide percentage has a daily (13%) or weekly (28%) use. The 48% of the analysed stock suffered damage during last earthquake (6 April 2009) and is currently not accessible (Fig. 5b).

As far as the urban context and the relation of the studied churches with the surrounding built environment are concerned, Fig. 6a shows that a low percentage (34%) is made of isolated churches (Fig. 6b), which generally are characterized by a lower structural vulnerability. On the contrary, many churches (66%) are somehow included in clusters of buildings (i.e. churches enclosed in historic aggregates, Fig. 6c, surrounded by shorter buildings, Fig. 6d, and located at the outer edge, Fig. 6e).

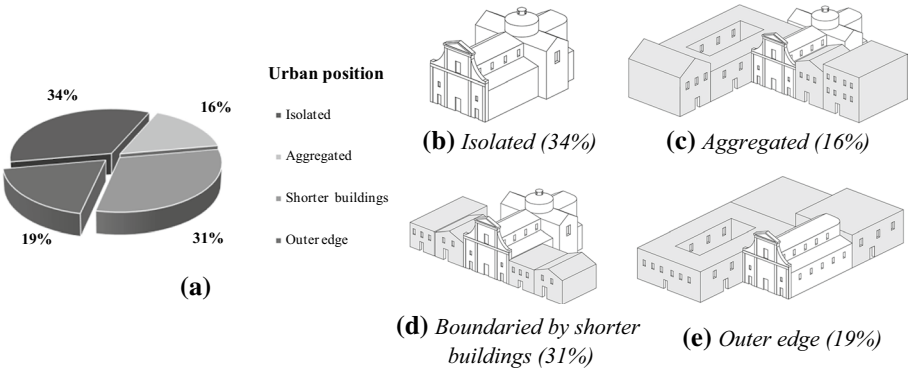

Fig. 6 Urban context of investigated churches

2.2 Classification according to foundation period

A classification of all churches in three different groups has been proposed, according to both the original foundation period and the succeeding transformations. This classification allows to recognise different structural features and therefore possible different seismic behaviours under seismic loading (churches of different vulnerability classes).

The first group refers to the *Medieval* churches, namely Romanesque and Gothic churches or, more generally, religious structures built by mendicant orders. These buildings are generally characterized by a simple plan covered by timber trusses, without transept and dome. The quality of masonry is generally good, because of a well refined fabric characterised by a regular pattern of stones. A significant example of this kind of structures is represented by St. Pietro ad Oratorium church in Capestrano [SPO; SU-VA], shown in Fig. 7. This group of churches is generally characterized by a good structural response with presence of few fragilities; thus, they can be classified as *Low Vulnerability Churches* [LV].

The second group is made of *Post-Medieval* churches, mainly built in Renaissance and Baroque periods. These are churches with a more complex plan, very often characterized by the presence of apses, transepts, vaults and domes. Masonry is generally made of heterogeneous and irregular rubble stones of variable sizes. A valuable example is represented by St. Maria Extra Moenia church in Petogna [SMX; AQ], shown in Fig. 8.

Post-Medieval churches are usually more vulnerable than the *Medieval* ones, because of the higher structural complexity and the poorer constructive quality. Thus, they can be classified as *Medium Vulnerability Churches* [MV].

The third group is made of the so-called *Hybrid* churches, which are characterized by heterogeneous structural and architectonic features. The significant stratifications detected in this type of churches, the difference between internal and external parts or even among different portions of the same sub-structures are strictly related to the high seismicity of Abruzzi. In fact, the several post-earthquake reconstructions occurred on structures very often involved the use of poor-quality constructive techniques (e.g. absence of connections between parts or lack of homogeneity in masonry) or of not adequate materials (e.g. concrete elements). An emblematic case is represented by St. Maria of Collemaggio church in L'Aquila [CLM; AQ], whose post-seismic condition is shown in Fig. 9. The presence of several stratifications makes this kind of structures particularly vulnerable, thereby they can be classified as *High Vulnerability Churches* [HV].

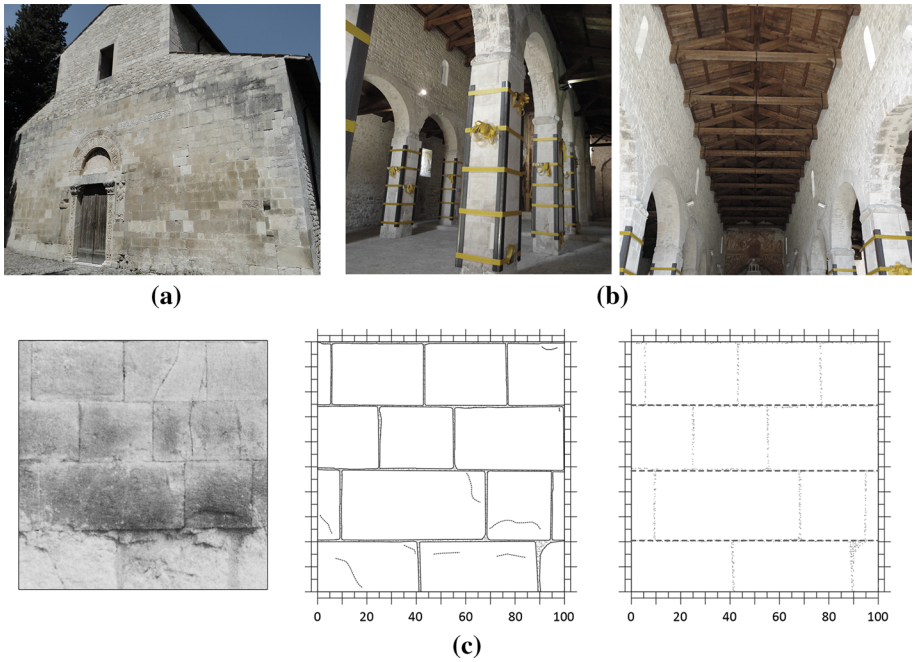

Fig. 7 External (**a**) and internal (**b**) details of St. Pietro ad Oratorium church in Capestrano [SU-VA]; masonry pattern (**c**)

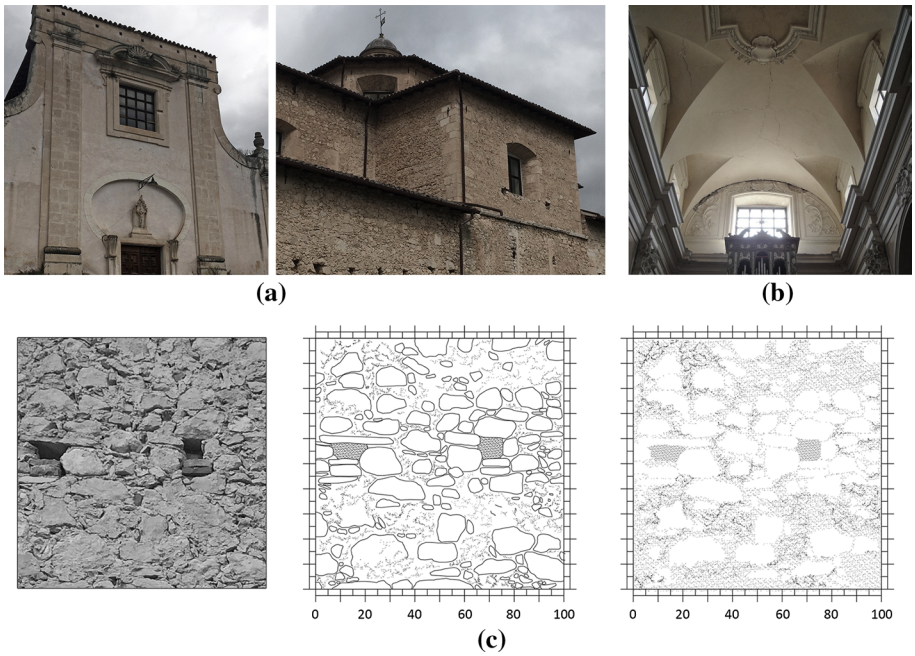

Fig. 8 External (**a**) and internal (**b**) details of St. Maria Extra Moenia church in Petogna [AQ]; masonry pattern (**c**)

Fig. 9 External (**a**) and internal (**b**) post-seismic state of St. Maria of Collemaggio church in L'Aquila [AQ]

Figure 10 shows the frequencies of the above defined vulnerability classes in the analysed stock. As it can be observed, a great percentage of the analysed churches (77%) belongs to HV class (*Hybrid* churches).

2.3 Distinctive features

Apart from the classification described above, a detailed analysis has been carried out also with regard to the applied constructive techniques and adopted materials. In particular, four different types of walls have been detected:

- Regular ashlar masonry with regular pattern (already shown in Fig. 7c);
- Rubble stones masonry with heterogeneous and irregular shapes and sizes (already shown in Fig. 8c);
- Semi-regular ashlar masonry, with semi-regular shapes and pattern. The so called *apparecchio aquilano* is a particular example of this type of masonry, made of semi-regular and square-shaped stones arranged in horizontal and parallel layers. Such a wall type, which was widely used in L'Aquila diocese since the 12th century, has been for example detected in St. Silvestro church in L'Aquila [SSV; AQ], shown in Fig. 11;
- Non-homogeneous masonry, with different and non-regular patterns and materials.

The frequencies of the aforementioned types of wall masonry for the considered churches are reported in Fig. 12, with reference to the façades (Fig. 12a), transepts (Fig. 12b), apses (Fig. 12c) and lateral walls (Fig. 12d). A prevalent frequency of

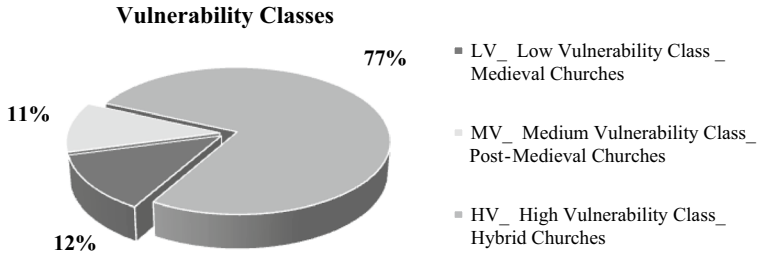

Fig. 10 Vulnerability classes for the investigated churches

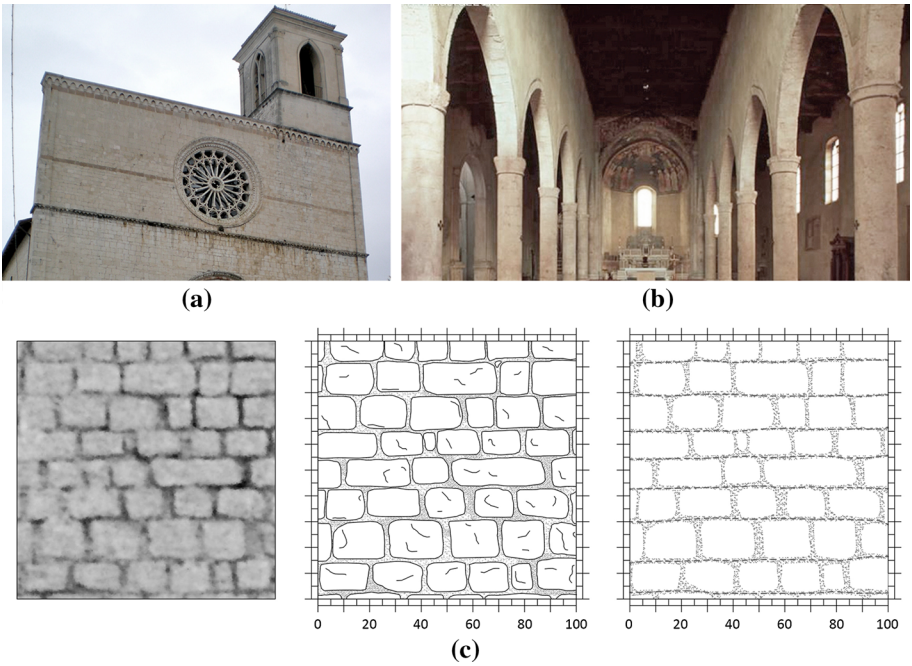

Fig. 11 External (**a**) and internal (**b**) details of St. Silvestro church in L'Aquila [AQ]; masonry pattern (*apparecchio aquilano*) (**c**)

rubble stone masonry can be observed in all cases, but a high percentage of regular ashlars masonry can be observed for façades (38% of the cases).

The observations carried out in the aftermath of L'Aquila seismic event allowed also to obtain more specific information about the internal structure of walls, which in many cases are composed by two parallel leaves without any transversal connections. Thus, the external leaf is lacking of constraint elements and is prone to undergo out-of-plane collapse due to delamination. This type of mechanism has been for example observed in the apse of St. Eusanio Martire church in S. Eusanio Forconese [SEU; AQ] after the 2009 L'Aquila earthquake (Fig. 13).

As far as the employed constructional materials are concerned, in L'Aquila district a clear prevalence of limestone has been detected. The use of marlstone, sandstone and clay has been observed only seldom. In addition, the use of lime mortar with rubble elements is typical of this territory; a wide presence of gravel can be also observed for buildings located near the rivers.

3 Structural features

3.1 General

From the structural point of view, historical buildings in seismic prone areas reflects the *local seismic culture* (D'Antonio 2013), namely that constructive practice made of

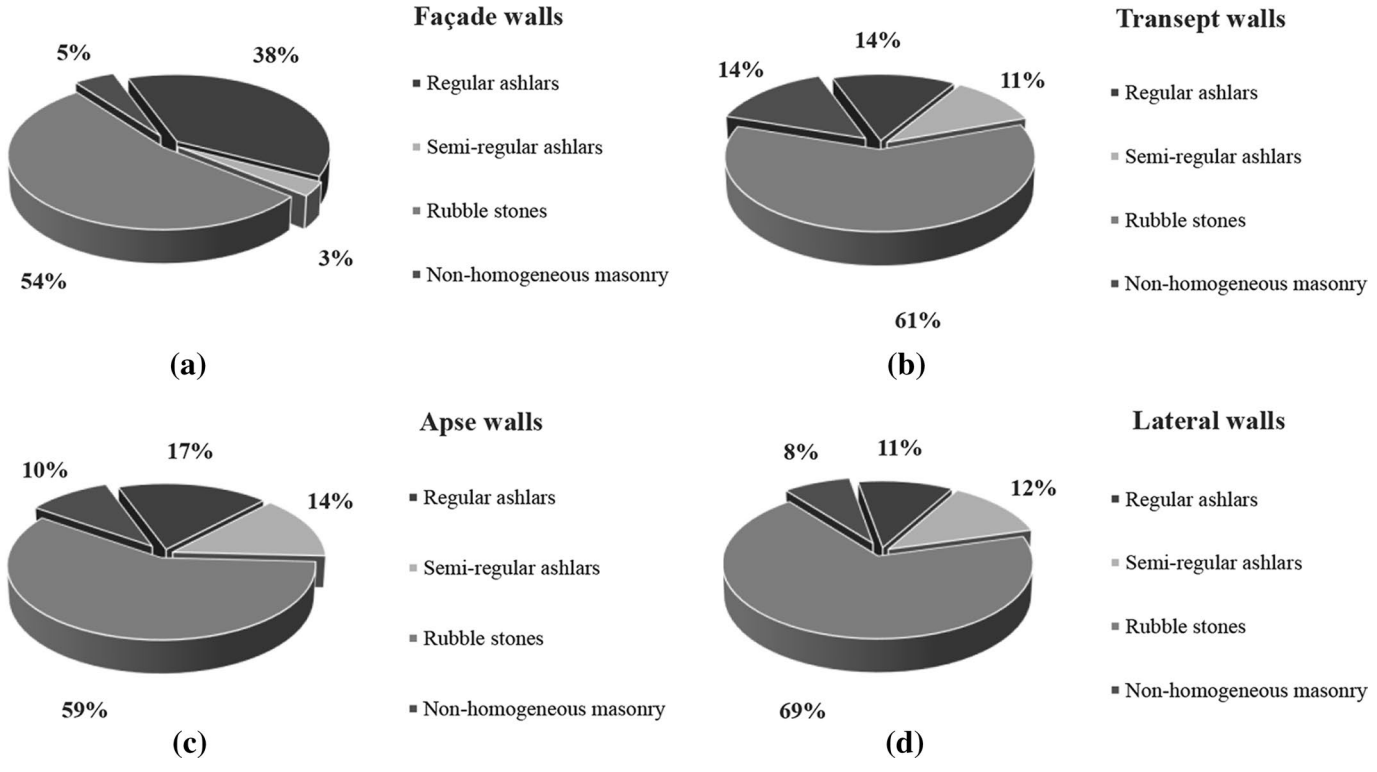

Fig. 12 Frequencies of masonry types

Fig. 13 Collapse mechanism detected in the apse of St. Eusanio Martire church in S. Eusanio Forconese [AQ]

empirical rules based on a sort of historical *trial and error* procedure. In fact, constructional details have been conformed in order to account for problems and criticalities evidenced after seismic events of the past: a clear example is represented by the use of wooden ties in masonry walls, such as the ones observed after the 2009 L'Aquila earthquake in the dome of St. Maria of Suffrage [AQ] (Fig. 14a).

In Abruzzi, the use of anti-seismic devices was significant in the 18th century, due to the earthquakes that stroke L'Aquila and Sulmona in 1703 and 1706, respectively, which determined the necessity to adopt adequate anti-seismic details and systems to mitigate potential damage.

On the other hand, the absence of strong earthquakes during the 19th century resulted in a loss of awareness and attention in adopting preventive solutions. For this reason, in the 20th century, traditional constructive techniques were *forgotten* and heavy structural alterations were carried out with modern and invasive materials. An example is the large use of bad-connected rigid reinforced concrete roofs on the original fabric, as in the case of the church of St. Maria of Paganica in L'Aquila [AQ] (Fig. 14b), fully collapsed after the last seismic event.

(a) **(b)**

Fig. 14 Wooden ties in the dome of St. Maria of Suffrage in L'Aquila [AQ] (**a**); rigid ring beams in St. Maria of Paganica in L'Aquila [AQ] (**b**)

Knowledge of historical constructive techniques and awareness of intrinsic features of buildings (adopted materials, presence/absence of anti-seismic devices, stratifications, etc.) are important for a reliable assessment of seismic vulnerability of masonry historical structures as well as to define possible suitable interventions, avoiding invasive and not adequate retrofitting solutions.

In the following, the main structural features of the analysed stock of churches are analysed. To this aim, the classification of structural elements that determine *anti-seismic* and *fragility* indicators for defining a vulnerability index for churches is provided.

3.2 Anti-seismic structural elements

The main anti-seismic devices observed in the considered stock of buildings are ties (longitudinal, transversal and ring ties), retaining elements (pilasters, buttresses, flying buttresses), corner connections and ring beams. They are schematically represented in Fig. 15, which, similarly to Figs. 18 and 21 (the last concerning the fragility indicators; see Sect. 3.3), has been drawn by the Authors on the basis of the list of possible anti-seismic devices reported in the Italian Guidelines for Cultural Heritage (2011). They have been observed according to the statistical data shown in Fig. 16.

In particular, longitudinal ties have been revealed at about half height of the façade (*first order*) in 16% of cases, at about two-third of the height of the façade (*second order*) for 25% of churches and at both first and second order in 13% of cases; ties has not been detected in façade for the 46% of the analysed churches.

Transversal ties have been observed in 16% of churches for lateral aisles walls (*first order*), in 13% of cases in central nave (*second order*), in 14% of churches at both first and second order; no transversal ties have been revealed in the remaining cases (57%). Transversal ties have been also observed in presbyteries (22%), transepts (50%), in the plane of façades (24%) and chapels (25%) when these macro-elements are present (in 100%, 44%, 98% and 6% of analysed churches, respectively).

A significant percentage of ties or ring ties has been also observed on domes (23%), bell towers (50%), bell cells (50%), for those cases where these macro-elements have been detected (in 48%, 68%, and 91% of the investigated churches, respectively). Figure 17a shows an example of transversal tie located in the plane of the façade of St. Sebastiano church in Navelli [SSB; AQ].

The observed frequencies of retaining elements—in particular, of transversal pilasters and buttresses (since flying buttresses have been detected in very few cases)—are shown in Fig. 16b, c, whereas Fig. 17b shows an example of transversal buttresses located at the first order of lateral walls in St. Maria della Valle church in Scanno [SMV; SU-VA].

Furthermore, as can be observed in Fig. 16d, a high percentage of effective transversal connections between walls has been detected in the analysed churches. Figure 17c shows the corner connection observed between walls in the façade of St. Pelino Basilica in Corfinio [SPE; SU-VA].

The analysis also concerned the presence/absence of elements that are not properly definable as anti-seismic devices, but representative of a good constructive practice, which is useful for reducing or avoiding collapse mechanisms activation. In particular, the survey focused on good connections between walls and roofs, correct geometric proportions, presence of structural elements and leaned buildings (only when they are not connected to churches and do not represent non-regularity elements).

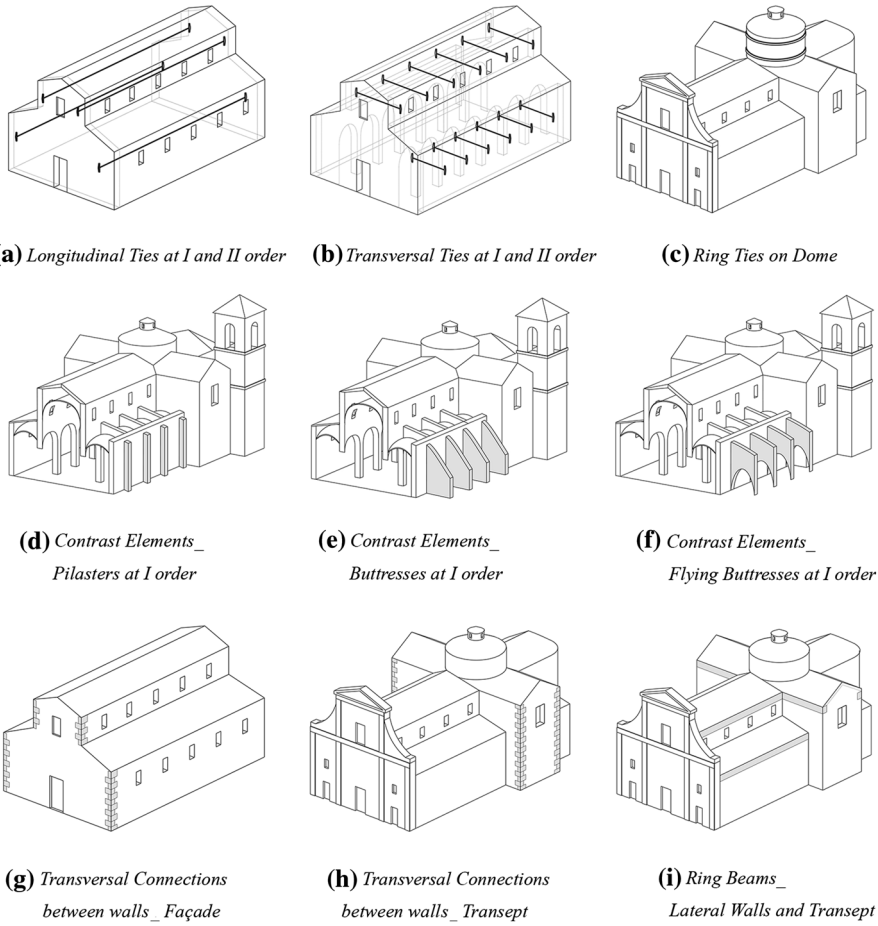

Fig. 15 Schematic representation of anti-seismic devices

Some examples of protective constructional elements are schematically represented in Fig. 18.

The observed frequencies of wall-to-roof connections and leaned buildings are shown in Fig. 19a, b, respectively. Figure 20a shows the example of lateral wall-to-roof connection observed in S. Maria Extra Moenia church in Petogna [SMX; AQ], whereas an example of leaned building on lateral walls is shown in Fig. 20b (St. Maria Maggiore church in Raiano [SMM; SU-VA]).

3.3 Fragility sources

As far as fragility sources are concerned, the survey focused on the presence of large openings (Fig. 21a), thrusting elements (i.e. thrusting roofs and vaults; Fig. 21b), heavy R.C. roofs (Fig. 21c), as well as on not adequate proportion of structural parts, asymmetry, irregularity, concentrated loads, presence of lunettes and light vaults.

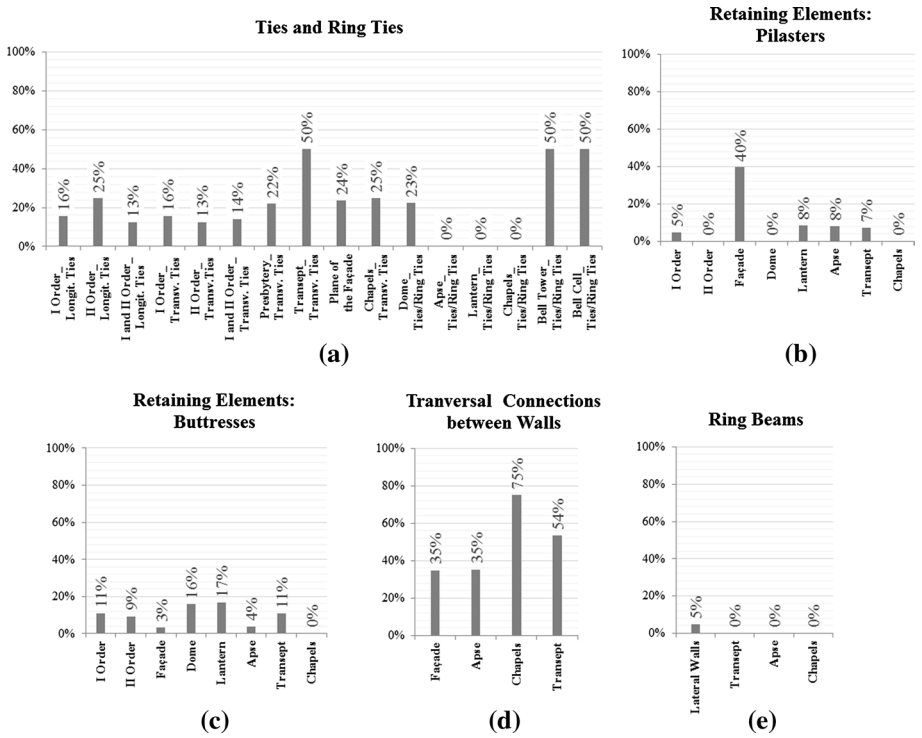

Fig. 16 Frequencies of anti-seismic devices

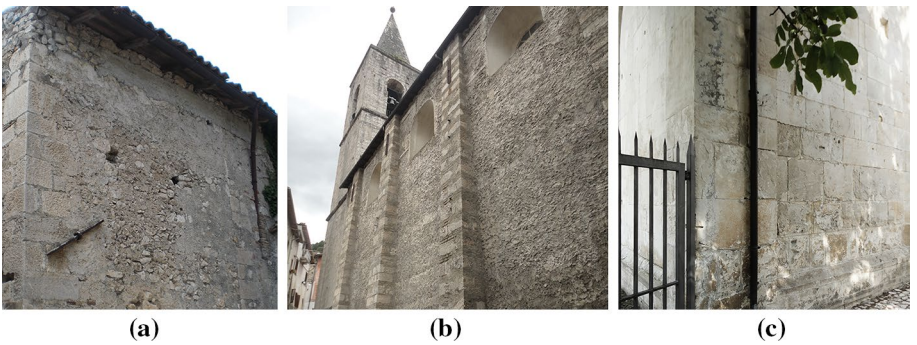

Fig. 17 Ties in the plane of the facade of St. Sebastiano church in Navelli [SSB; AQ] (**a**); transversal buttresses in lateral walls (I order) in St. Maria della Valle church in Scanno [SMV; SU-VA] (**b**); corner connection between walls in the façade of St. Pelino Basilica in Corfinio [SPE; SU-VA] (**c**)

In particular, earthquakes of the past generally showed that when heavy R.C. roofings were added on churches, often without effective connections with other existing elements, severe damage occurred, mainly due to the increased seismic weight, proving, contrarily to what was wrongly believed in the last century, that the presence of this intervention has to be intended as an added source of fragility.

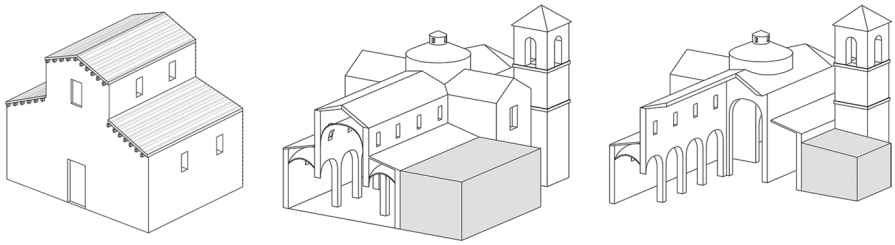

(a) *Façade-Roof Connection* **(b)** *Building on Lateral Walls* **(c)** *Building on Triumphal Arch*

Fig. 18 Schematic representation of protective constructional elements

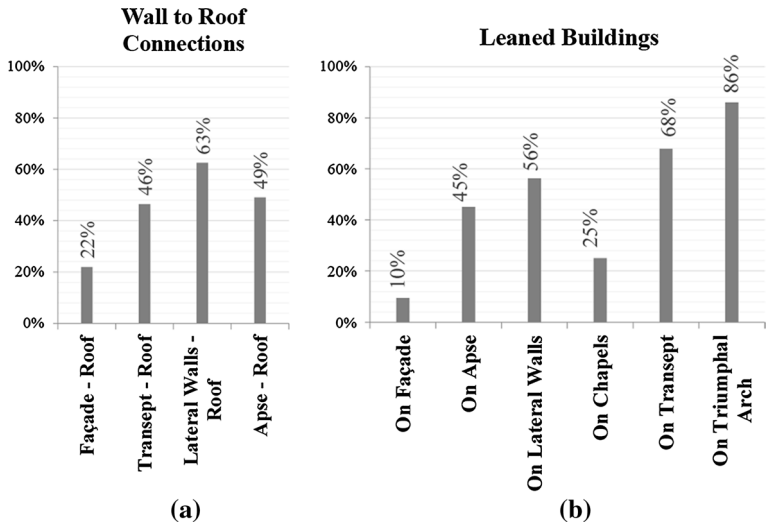

Fig. 19 Revealed frequencies of connections (**a**) and leaned buildings (**b**)

(a) **(b)**

Fig. 20 Lateral wall-roof connection in S. Maria Extra Moenia church in Petogna [SMX; AQ] (**a**); building leaned on lateral walls in S. Maria Maggiore church in Raiano [SMM; SU-VA] (**b**)

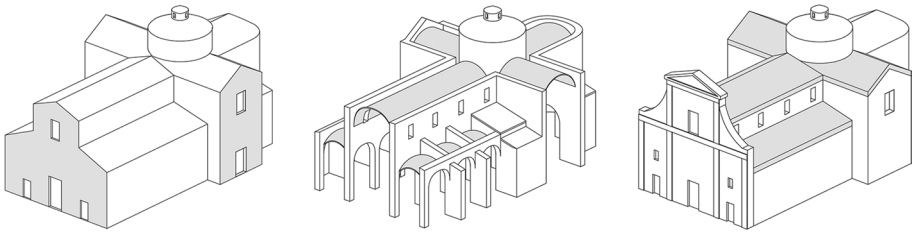

(a) *Openings in Facade and Transept* **(b)** *Thrusting Covering on Naves, Transept and Apse* **(c)** *Heavy R.C. Roof on Naves and Transept*

Fig. 21 Schematic representation of fragility sources

The frequencies of the considered features in the analysed population of churches are shown in Fig. 22, which particularly focuses on openings, thrusting coverings and R.C. roofs. It can be observed that a large percentage of openings has been detected in chapels (100%), façade (95%), lateral walls (86%), apse (82%), top of the transept (82%) and the top of the façade (78%). A significant percentage of thrusting elements (mainly referring to thrusting vaults) has been observed in apse (76%), transept (75%) and naves (66%), while a not negligible percentage of R.C. roofs (including R.C. ring beams) has been observed in transept (18%), central (13%) and lateral naves (14%).

In Fig. 23 some examples are shown: Fig. 23a refers to wide openings observed in the façade of St. Maria Assunta church in Assergi (L'Aquila) [SAN; AQ]; Fig. 23b shows the case of barrel vaults observed in the central nave of St. Panfilo cathedral in Sulmona [SPA; SU-VA]; Fig. 23c shows the case of St. Biagio of Amiternum church [SBM; AQ], with reference to heavy R.C. roof observed on naves.

4 Damage observation

A damage reconnaissance was carried out in the aftermath of the 2009 L'Aquila earthquake on churches belonging to both the analysed dioceses. More precise details on this activity are given in De Matteis et al. (2016). The damage analysis has been conducted according to the

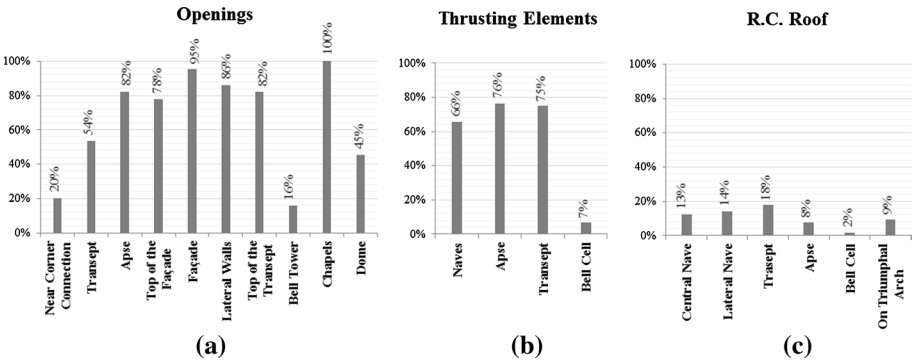

Fig. 22 Revealed frequencies of fragility sources

(a) **(b)** **(c)**

Fig. 23 Large openings in the façade of St. Maria Assunta church in Assergi [SAN; AQ] (**a**); thrusting vaults in St. Panfilo cathedral in Sulmona [SPA; SU-VA] (**b**); R.C. roof in St. Biagio d'Amiterum church in L'Aquila [SBM; AQ] (**c**)

procedure proposed in the Italian Guidelines on Cultural Heritage (2011). Therefore, a global damage index (i_d), defined by Eq. (1), as an integer number ranging from 0 (no damage) to 1 (full damage), has been assigned to each church according to engineeristic judgements. To this purpose all macro-elements of the church have been inspected separately.

$$\mathrm{i_d} = \frac{1}{5} \cdot \frac{\sum_{\mathrm{k}=1}^{28} \rho_{\mathrm{k,i}} \cdot \mathrm{d_{k,i}}}{\sum_{\mathrm{k}=1}^{28} \rho_{\mathrm{k,i}}} \tag{1}$$

In the above equation, for the generic kth macro-element that could experience a kinematic mechanism (with k ranging from 1 to 28), d_k represents the specific level of damage ($0 \le d_k \le 5$), which has been defined according to the criteria introduced by Grunthal (1998). In the same equation, ρ_k is a factor that weights the damage of the mechanism k according to the importance that such a mechanism has on the global stability of the church. The considered values are given by the Italian Guidelines (2011) and are reported in Fig. 24.

Then, the damage index i_d has been related to a damage score D_k ranging from 0 (no damage) to 5 (total collapse), according to the criterion provided by Lagomarsino and Podestà (2004b) shown in Table 1.

Finally, the frequency of each damage score D_k has been gathered in terms of Damage Probability Matrices (DPMs) as shown graphically in Fig. 25. The mean damage level for all examined churches ($\mu_{D,o}$) can be calculated according to Eq. (2), where n is the total number of churches.

$$\mu_{D,o} = \frac{\sum_{i=1}^{n} D_{k,i}}{n} \tag{2}$$

For the case being, $\mu_{D,o}$ resulted equal to 1.73. This value can be used in the Binomial Probability Distribution Function (BPDF) given in Eq. (3) and depicted also in Fig. 25 for comparison with the specific observed damage levels.

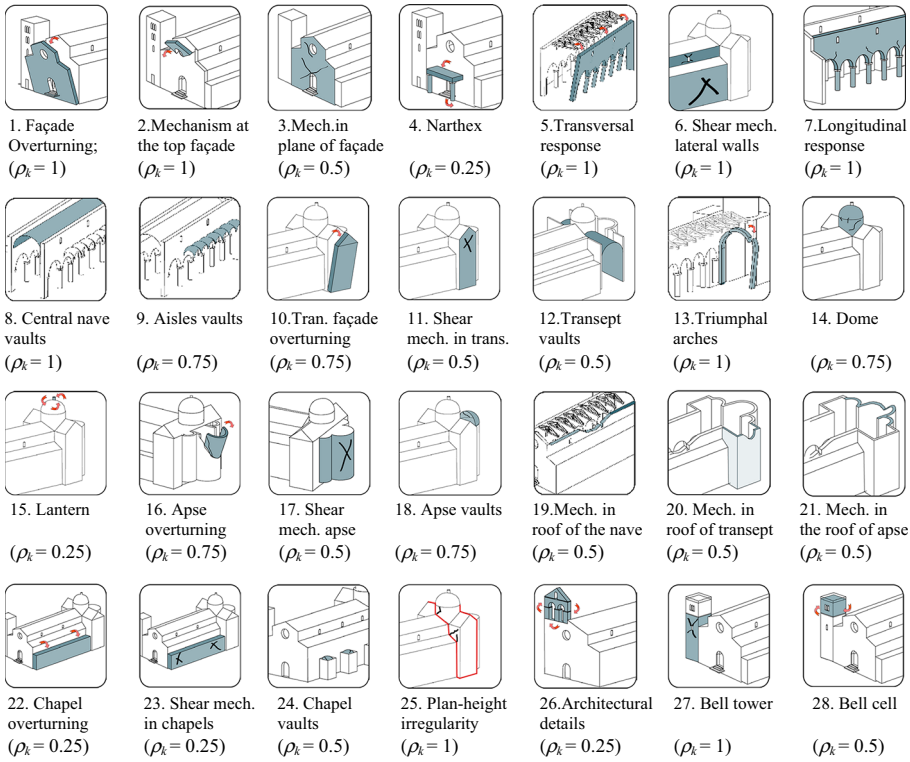

Fig. 24 Classification of mechanisms for religious buildings according to Guidelines for Cultural Heritage (2011)

Table 1 Correlation between damage indices i_d and damage scores D_k, (Lagomarsino and Podestà 2004b)

Damage score (D_k)	Damage index (i_d)	Description
D_0	$i_d \leq 0.05$	No damage
D_1	$0.05 < i_d \leq 0.25$	Negligible to slight damage
D_2	$0.25 < i_d \leq 0.4$	Moderate damage
D_3	$0.4 < i_d \leq 0.6$	Substantial to heavy damage
D_4	$0.6 < i_d \leq 0.8$	Very heavy damage
D_5	$i_d > 0.8$	Complete collapse

$$p_k = \frac{5!}{k!(5-k)!)}\left(\frac{\mu_{D,o}}{5}\right)^k\left(1-\frac{\mu_{D,o}}{5}\right)^{5-k} \tag{3}$$

It is apparent that the BPDF fits satisfyingly the frequencies of observed damage for the whole group of churches, even though without considering explicitly the occurred earthquake intensity church by church.

However, some discrepancies can be noticed for damage D1, D2 and D3. The discrepancies related to damage level D1 could be due to the fact that, in case of slight damage, it

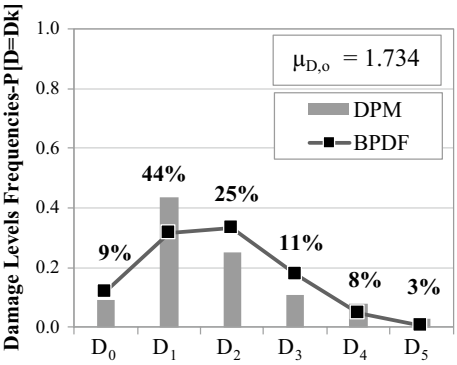

Fig. 25 Damage probability matrices (DPM) and binomial distribution function (BPDF) for the 64 observed churches

is quite difficult to distinguish between pre-existing cracks and the cracks provoked by the earthquake. This means that in some cases the observed damage D1 could have been overestimated at the expense of the evaluation of the damage D0.

On the other hand, the discrepancies observed for damage D2 and D3, which however appear to be acceptable, are probably due to the difficulties of precisely predict a damage scenario involving a so large territorial area. For example, the binomial distribution slightly underestimates the observed damage D4 and D5, probably at the expense of D3, because of some site effects that provoked the full development of mechanisms instead of their trigger.

In order to better interpret the above results, the same procedure has been applied to separate groups of churches hit by the same earthquake intensity I_{MCS}. To this purpose, three groups of churches have been considered according to the related macro-seismic intensity (I_{MCS} 5–5.5, I_{MCS} 6–6.5 and I_{MCS} 8). The related results are shown in Fig. 26. A good agreement of results can be observed especially for higher damage levels. The discrepancies between DPM and BPDF for lower damage levels, which are more widespread for low earthquake intensities, could be attributed to the fact that, in such cases, the ambiguities in classifying the pre-existing and the provoked damage could be more influential, this leading to higher estimated damage for higher damage levels.

The obtained results for high seismic intensity prove that the proposed model is extremely effective for earthquakes of high intensity, for instance $I_{MCS} = 8$, whereas

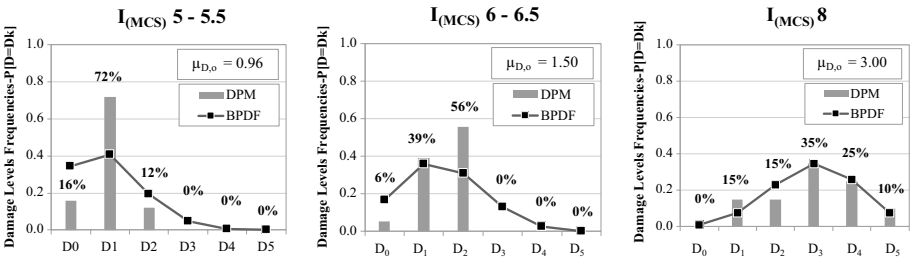

Fig. 26 Damage probability matrices (DPM) and binomial distribution function (BPDF) for separate groups of churches according to I_{MCS}

some issues arise for lower intensities, with some consequences on the global results shown in Fig. 25.

5 Predictive method

5.1 Vulnerability assessment procedure

In the following, an empirical methodology to evaluate potential post-seismic damage scenarios is presented.

The procedure exploits the definition of a vulnerability index, which is assigned according to the Eq. (4), as suggested by the Italian Guidelines (2011), but the procedure proposed in this paper is based on more comprehensive and objective criteria for the definition of the scores that contribute to define the vulnerability index i_v.

$$i_v = \frac{1}{6} \cdot \frac{\sum_{k=1}^{28} \rho_{k,i}(v_{k,i} - v_{k,p})}{\sum_{k=1}^{28} \rho_{k,i}} + \frac{1}{2} \tag{4}$$

In the above equation, for the generic kth mechanism (with k ranging from 1 to 28), v_{ki} and v_{kp} are scores that can be ascribed to the fragility indicators and to the anti-seismic devices, respectively, while ρ_k is the importance factor, already used in Eq. (1) and provided in Fig. 24.

The evaluation of each score of v_{ki} and v_{kp} has been carried out according to Eqs. (5) and (6), respectively, which are implemented by defining specific factors (z, w, f and η) in order to make the evaluation less subjective than those carried out in previous studies (Brando et al. 2017).

$$v_{k,i} = \sum_{i=1}^{n} z \cdot w \cdot f \tag{5}$$

$$v_{k,p} = \sum_{i=1}^{n} z \cdot w \cdot \eta \tag{6}$$

In the above equations, z is a Boolean coefficient, which can be equal to 1 or 0, depending on the presence/absence of the fragility indicators and protection devices, in Eqs. (5) and (6), respectively. The w coefficient is an importance factor ranging from 0 to 2. In Eq. (5) it represents the potentiality of the fragility source associated to the indicator to determine the vulnerability of the mechanism, while in Eq. (6) it is a measure of the capability of the applied protection device typology for inhibiting or limiting the mechanism development. For example, large openings or heavy roofs located at the top of the walls are supposed to be equally important in influencing or worsening in plane behaviour of walls. Similarly, contrast elements or ties may have a different importance in inhibiting the out-of-plane mechanisms of a macro-element (i.e. façades, transepts, apses) as well as

longitudinal or transversal ties may have a different importance in inhibiting overturning mechanisms if they are placed at I or II order in the considered structures.

The fragility factor f in Eq. (5) measures the effectiveness of the indicator and ranges from 0 (meaning that the indicator does not influence the activation of mechanism) to 1.5, in case of full influence on the onset of the same mechanism. Analogously, the efficiency factor η in Eq. (6) measures the effectiveness of the anti-seismic system that mitigates the possible failure. It also ranges from 0 to 1.5.

As an example, in the out of plane mechanism of the façade, the detectable anti-seismic devices are: transversal connections between walls, *I* and *II order* longitudinal ties, contrast elements and leaned buildings. For transversal connections between walls, the w coefficient is set to 0.75, considering their effectiveness in inhibiting the overturning mechanism. If transversal connections are actually present, the Boolean coefficient z is fixed equal to 1. The efficiency factor η is set to 1.5 in case of totally effectiveness of the device, to 1 in case of its partially effectiveness.

In the same mechanism, the detectable fragility indicators are: presence of openings at the corner and presence of thrusting elements. For the openings at the corner, w is set to 1.5 (considering the influence of the fragility indicator on the onset of the mechanism), z is fixed to 1 in case of presence. The fragility coefficient f is set to 1.5 in case of large openings presence, to 1 if smaller openings are detected.

The described methodology has been applied to the investigated churches, figuring out a situation in which no damage has occurred. The obtained vulnerability indices i_v are shown in Fig. 27. The mean value $\underline{i}_v$ is equal to 0.568.

In the considered stock of churches, lower vulnerability indices i_v have been obtained for San Pelino church [SPE; $i_v = 0.422 -$ LV class -] in Corfinio and for San Pietro Celestino church [SPC; $i_v = 0.422 -$ MV class -] in Pratola Peligna. San Pelino church was built in the 11th century and preserves the Romanesque style restored during the 1970s. The construction is characterized by a latin-cross plan (with transept and apse) covered by timber trusses, without vaults and dome. The quality of masonry is good, thanks to the regular texture (regular ashlar masonry). The low value of i_v is therefore related to the good quality of constructive techniques and to the absence of fragility indicators. This structure suffered very slight damage during the 2009 L'Aquila earthquake ($i_d = 0.039$; $I_{MCS} = 6$).

On the contrary, the highest value of i_v has been determined for Ss. Nicandro and Marciano church [SNM; $i_v = 0.705 -$ HV class -] in Roio Piano (L'Aquila). The church, built in the 12th century and characterized by successive reconstructions, has a basilica layout (with no transept and apse) covered by thin vaults in the central nave. The masonry is made of rubble stones with non-regular shapes and sizes. The high structural vulnerability is therefore related to the poor quality of constructive techniques as well as to the presence of fragility indicators (such us concrete ring beams on lateral walls) and to the almost total

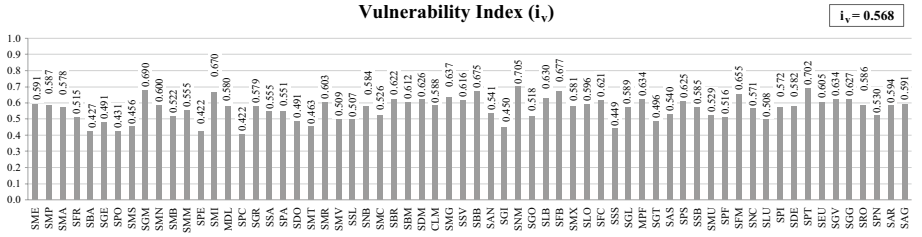

Fig. 27 Vulnerability indices i_v for the 64 three naves churches of Sulmona-Valva and L'Aquila dioceses

Table 2 Vulnerability indices $\overline{i_v}$ and damage indices $\overline{i_d}$ for churches of low, medium and high vulnerability class

Vulnerability class	Vulnerability index ($\overline{i_v}$)	Damage index ($\overline{i_d}$)
Low vulnerability (LV)	0.468	0.110
Medium vulnerability (MV)	0.542	0.199
High vulnerability (HV)	0.553	0.336

absence of anti-seismic devices (ties have been detected only in bell cell and bell tower). This structure suffered heavy damage during the 2009 seismic event (i_d=0.829; I_{MCS}=8).

Table 2 provides the obtained mean values of vulnerability indices $\overline{i_v}$ for the vulnerability classes of churches defined in Sect. 2. A higher vulnerability has been generally observed in churches characterized by more complex structures and lower constructive quality (in particular in HV churches, characterized by several post-seismic reconstructions).

In the same table, the mean damage indices $\overline{i_d}$, defined for each church by applying Eq. (1), are also provided. A higher value of $\overline{i_d}$ is associated to groups of churches characterized by a higher vulnerability class.

5.2 Predictive versus observed damage

The mean vulnerability index $\overline{i_v}$, resulting by the application of the above method, has been used to define the expected mean damage $\mu_{D,p}$ ($\overline{i_v}$) of the studied churches for several earthquakes of macro-seismic intensity I_{MCS} ($0 \le I_{MCS} \le 12$), through the application of the vulnerability function given by Lagomarsino and Podestà (2004b) and reported in Eq. (7).

$$\mu_{d,p} = 2.5\left[1 + \tanh\left(\frac{I + \alpha \cdot \overline{i_v} - \gamma}{\beta}\right)\right] = 2.5\left[1 + \tanh\left(\frac{I + 3.4375 \cdot \overline{i_v} - 8.9125}{3}\right)\right] \quad (7)$$

The adopted function provides the mean damage level $\mu_{D,p}$ as a function of earthquake intensity I (measured in the Mercalli-Cancani-Sieberg scale) and the mean vulnerability index $\overline{i_v}$ defined for the considered group of churches.

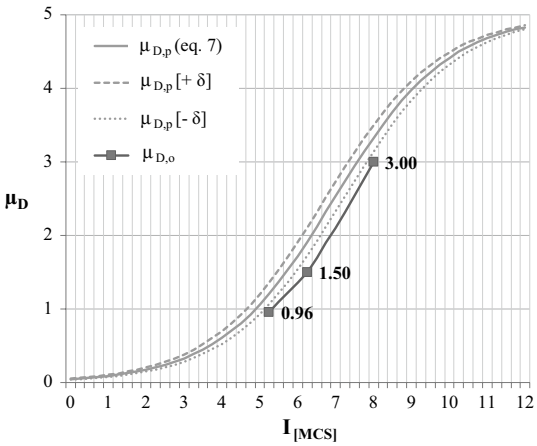

Fig. 28 Mean damage values versus macro-seismic intensity: comparison between Eq. (7) and observed values

In Fig. 28, the corresponding vulnerability function is given: the values of the expected mean damage $\mu_{D,p}$ are assessed for different earthquake intensities and compared to the values of mean damage $\mu_{D,o}$, observed for the three groups of churches defined in Sect. 4 (I_{MCS} 5–5.5, I_{MCS} 6–6.5 and I_{MCS} 8) and evaluated according to Eq. (2). In the same figure, the curves obtained by increasing and reducing the values $\mu_{D,p}(\overline{i_v})$ by the standard deviation δ, computed according to Eq. (8), are also shown.

Although the existing predictive method appears to be conservative, a certain scatter between observed and predicted damage levels can be noted when Eq. (7) is used. Moreover, the observed values of mean damage are not included in the fuse formed by the curves obtained by increasing and decreasing the mean damage by the standard deviation δ. For this reason, the expression given in Eq. (7) has been adjusted in order to fit satisfactorily the damage actually observed for the churches under investigation.

The graphs given in Fig. 29 shows that the parameters α (=3.4375) and γ (=8.9125) in the numerator and

$$\delta = \sqrt{\frac{\sum_{i=1}^{n}\left(i_{v,i} - \overline{i_v}\right)^2}{n}} \tag{8}$$

β (=3) in the denominator of Eq. (7) control the shape of the vulnerability curve. In particular, the parameter β, which is usually related to the ductility of the constructions, controls the flexure of the curve. It is evident that smaller values of β (<3) produce curves with a larger variation of the slope. Constructions characterized by such a behaviour suffer damage that changes rapidly when the earthquake intensity varies. On the contrary, larger values of β (>3) produce curves with a less pronounced flexure, reflecting an opposite behaviour. For β=3 the slope of vulnerability curve seems to be consistent with the trend of the mean damage values observed for the analysed churches.

On the other hand, the variation of the parameters α and γ produces a shift of the vulnerability curve.

All the above considerations lead to address the fitting procedure to the modification of the parameters α and γ only, aiming at reducing the scatters between the observed and the predicted mean damage shown in Fig. 28.

The modified vulnerability function is given in Eq. (9).

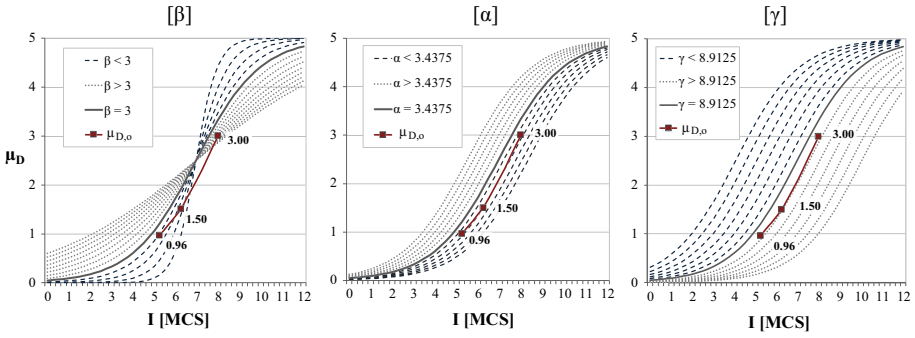

Fig. 29 Effect of β, α and γ parameters on the shape of vulnerability curves

$$\mu_{D,p} *= 2.5\left[1+\tanh\left(\frac{I+6.20\cdot\overline{i_v}-11}{3}\right)\right] \tag{9}$$

The new comparison between predicted and observed damage levels is proposed in Fig. 30. It can be noted that the vulnerability function given by Eq. (9) fits very well the results coming from the in-field survey carried out after the 2009 L'Aquila Earthquake. This means that the implemented modifications allow to get more realistic and reliable results, at least for the typology of churches considered in this paper.

It has been also found that a more precise fitting between the observed mean damage and the predicted one is given if the stock of churches is divided according to groups experiencing the same macro-seismic intensity.

As a matter of fact, the vulnerability indices of the churches belonging to the three separate groups characterized by churches which undergone the same macro-seismic intensity have been evaluated (Table 3).

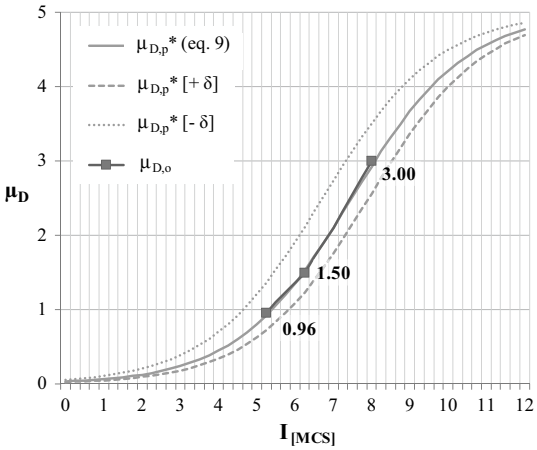

Fig. 30 Mean damage values vs macro-seismic intensity: comparison between Eq. (9) and observed values

Table 3 Vulnerability indices $\overline{i_v}$ for the three groups of churches (I_{MCS}5–5.5, 6–6.5 and 8)

Group of churches	Vulnerability index $(\overline{i_v})$
I_{MCS} 5–5.50	0.535
I_{MCS} 6–6.50	0.546
I_{MCS} 8	0.603

Table 4 Mean damage values for the three groups of churches (IMCS5–5.5, IMCS 6–6.5 and IMCS 8)

Groups of churches	$\mu_{D,p,MCS}$—Eq. (7)	$\mu_{D,p}{}^{*}{}_{,MCS}$—Eq. (9)
I_{MCS} 5–5.50	1.143	0.824
I_{MCS} 6–6.50	1.861	1.437
I_{MCS} 8	3.421	3.103

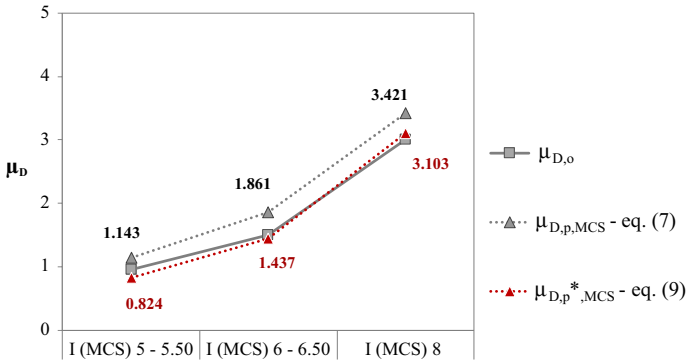

Fig. 31 Mean damage values vs macro-seismic intensity for the three groups of churches (I_{MCS}5–5.5, I_{MCS} 6–6.5 and I_{MCS} 8)

By using these values, both Eqs. (7) and (9) have been applied and the corresponding mean damage ($\mu_{D,p,MCS}$) associated to each macro-seismic intensity has been determined (Table 4). For the sake of comparison, the obtained values can be compared to the observed mean damage levels ($\mu_{D,o}$) reported in Fig. 26. The above comparison is also provided in Fig. 31, where both observed and predicted mean damage values are represented. It appears that a very good agreement is obtained when Eq. (9) is applied.

5.3 Fragility curves

The proposed vulnerability function provided in Eq. (9) can be used to define fragility curves which correspond to possible damage scenario related to several macro-seismic intensities ($0 \le I_{MCS} \le 12$). To this purpose, the mean vulnerability index $\overline{i_v}$ defined for the whole population of churches has been used in order to define the expected mean damage $\mu_{D,p}$ for each intensity I_{MCS} ($0 \le I_{MCS} \le 12$) through the application of Eq. (9). Therefore, the Binomial Function (BPDF) given in Eq. (3) has been used to draw fragility curves, which represent the probability of exceeding a certain level of damage [$P(D \ge D_k) = \sum_{j=k}^{5} p_j$; with $1 \le D_k \le 5$], as a function of the macro-seismic intensity I_{MCS}, considering the value of the expected mean damage given by Eq. (9).

The obtained fragility curves are shown in Fig. 32, where the same curves obtained by applying Eq. (7), for the same vulnerability index, are also plotted. The curves obtained by applying the proposed formulation are evidently less conservative and this aspect could be related to the fact that the stock of churches considered in the study, differently by previous studies in the literature, is characterized by more homogenous plans.

6 Conclusions

In this paper a predictive methodology for the vulnerability assessment of churches at territorial scale has been presented.

The method, which results from some modifications applied to literature procedure and largely applied in the past, has been calibrated on the basis of the damage observed after

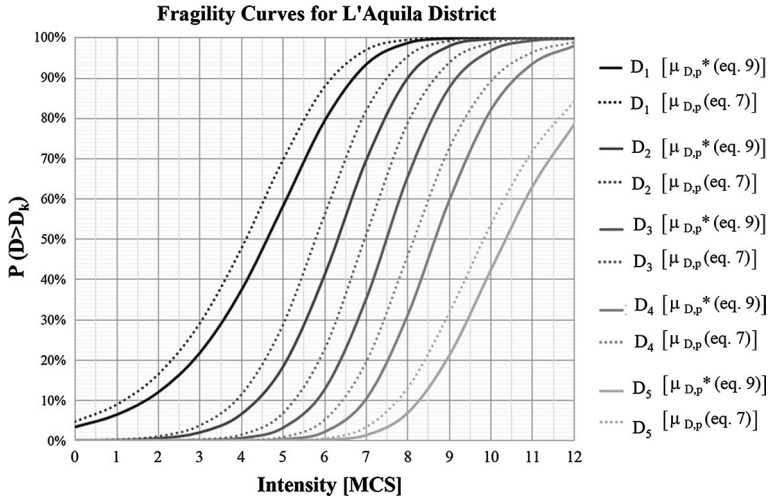

Fig. 32 Fragility curves

the 2009 L'Aquila earthquake on the 64 three naves churches of the two dioceses of Sulmona-Valva and L'Aquila.

The following main conclusions can be drawn out:

1. The analysed stock of churches can be subdivided in three vulnerability classes: *Low*, *Medium* and *High* Vulnerability classes; the most vulnerable churches are the ones that undertook significant transformations during their life, herein defined as *Hybrid* churches;
2. For the same earthquake intensity, higher damage has been generally observed for churches characterized by higher vulnerability indices, this meaning that the way of calculating these indices is able to reproduce the real fragilities of churches when subjected to earthquakes;
3. The observed damage scenarios of analysed churches have been satisfyingly fitted by the binomial distribution, provided by Eq. (3), especially when applied to churches having suffered more severe damage or belonging to areas that experienced higher macro-seismic intensities;
4. The vulnerability function provided in Eq. (9), which has been proposed by modifying some coefficients of the previous vulnerability function—Eq. (7)—provided by Lagomarsino and Podestà (2004b), allows to get realistic results and a precise fitting between observed and predicted damage, especially when separate stocks of churches are considered according to the experienced macro-seismic intensity.
5. The fragility curves obtained through the application of the new vulnerability function, are less conservative than the ones obtained by the application of Eq. (7). Probably, this result is due to the fact that the stock of churches considered in this study is characterized by more homogenous plans.

Therefore, the vulnerability function proposed in this study could be adopted to define reliable fragility curves that can be used for predicting possible damage scenarios at large

territorial area of churches having constructional features similar to ones analysed in this paper.

References

Betti M, Borghini A, Boschi S, Ciavattone A, Vignoli A (2018) Comparative seismic risk assessment of basilica-type churches. J Earthq Eng 22(supl1):62–95. https://doi.org/10.1080/13632469.2017.1309602

Brando G, Criber E, De Matteis G (2015) The effects of L'Aquila earthquake on the St. Gemma church in Goriano Sicoli: part II-fem analysis. Bull Earthq Eng 13(12):3733–3748. https://doi.org/10.1007/s10518-015-9793-3

Brando G, De Matteis G, Spacone E (2017) Predictive model for the seismic vulnerability assessment of small historic centres: application to the inner Abruzzi Region in Italy. Eng Struct 153:81–96. https://doi.org/10.1016/j.engstruct.2017.10.013

Brandonisio G, Lucibello G, Mele E, De Luca A (2013) Damage and performance evaluation of masonry churches in the 2009 L'Aquila earthquake. Eng Fail Anal 34:693–714. https://doi.org/10.1016/j.engfailanal.2013.01.021

Criber E, Brando G, De Matteis G (2015) The effects of L'Aquila earthquake on the St. Gemma church in Goriano Sicoli: part I-damage survey and kinematic analysis. Bull Earthq Eng 13(12):3713–3732. https://doi.org/10.1007/s10518-015-9792-4

Da Porto F, Da Silva B, Costa C, Modena C (2012) Macro-scale analysis of damage to churches after earthquake in Abruzzo (Italy) on April 6, 2009. J Earthq Eng 16(6):739–758. https://doi.org/10.1080/13632469.2012.685207

D'Antonio M (2013) Ita terraemotus damna impedire. Note sulle tecniche antisismiche storiche in Abruzzo. EAN: 9788850103195 Ed. Carsa, Pescara, 24 p., ill., Brossura

D'Ayala D (2000) Establishing correlation between vulnerability and damage survey for churches. In: Proceedings of 12th world conference on earthquake engineering, New Zealand, January–February 2000, paper 2237

D'Ayala D (2005) Force and dispacement based vulnerability assessment for traditional buildings. Bull Earthq Eng 3(3):235–265. https://doi.org/10.1007/s10518-005-1239-x

De Matteis G, Mazzolani FM (2010) The Fossanova church: seismic vulnerability assessment by numerical and physical testing. Int J Arch Heritage 4(3):222–245. https://doi.org/10.1080/15583050903078903

De Matteis G, Zizi M (2019) Seismic damage prediction of masonry churches by a PGA-based approach. Int J Arch Heritage. https://doi.org/10.1080/15583058.2019.1597215

De Matteis G, Criber E, Brando G (2016) Damage probability matrices for three-nave masonry churches in Abruzzi after the 2009 L'Aquila Earthquake. Int J Arch Heritage 10(2–3):120–145. https://doi.org/10.1080/15583058.2015.1113340

De Matteis G, Corlito V, Guadagnuolo M, Tafuro A (2019a) Seismic vulnerability assessment and retrofitting strategies of italian masonry churches of the Alife-Caiazzo Diocese in Caserta. Int J Arch Heritage. https://doi.org/10.1080/15583058.2019.1594450

De Matteis G, Brando G, Corlito V, Criber E, Guadagnuolo M (2019b) Seismic vulnerability assessment of churches at regional scale after the 2009 L'Aquila earthquake. Int J Mason Res Innov 4(1–2):174–196

Del Gaudio C, Di Domenico M, Ricci P, Verderame G (2018) Preliminary prediction of damage to residential buildings following the 21st August 2017 Ischia earthquake. Bull Earthq Eng 16(10):4607–4637. https://doi.org/10.1007/s10518-018-0368-y

Doglioni F, Moretti A, Petrini V (1994) Le chiese e il terremoto—Dalla vulnerabilità constatata nel terremoto del Friuli al miglioramento antisismico nel restauro, verso una politica di prevenzione. Edizioni Lint., Trieste, Italy, ISBN: 8886179367

Faccioli E, Pessina V, Calvi GM, Borzi B (1999) A study on damage scenarios for residential buildings in Catania city. J Seismol 3(3):327–343. https://doi.org/10.1023/a:1009856129016

Giovinazzi S, Lagomarsino S (2004) A macroseismic model for the vulnerability assessment of buildings. In: Proceedings of 13th world conference on earthquake engineering. Vancouver, Canada, paper 896 (CD-Rom)

Grunthal G (1998) European Macroseismic Scale, Centre Européen de Géodynamique et de Séismologie, Luxembourg 1998; vol 15

Hofer L, Zampieri P, Zanini MA, Faleschini F, Pellegrino C (2018) Seismic damage survey and empirical fragility curves for churches after the August 24, 2016 Central Italy earthquake. Soil Dyn Earthq Eng 111:98–109. https://doi.org/10.1016/j.soildyn.2018.02.013

Lagomarsino S (2012) Damage assessment of churches after L'Aquila earthquake (2009). Bull Earthq Eng 10(1):73–92. https://doi.org/10.1007/s10518-011-9307-x

Lagomarsino S, Podestà S (2004a) Seismic vulnerability of ancient churches: I. Damage assessment and emergency planning. Earthq Spectra 20(2):377–394. https://doi.org/10.1193/1.1737735

Lagomarsino S, Podestà S (2004b) Seismic vulnerability of ancient churches: II. Statistical analysis of surveyed data and methods for risk analysis. Earthq Spectra 20(2):395–412. https://doi.org/10.1193/1.1737736

Lagomarsino S, Podestà S (2004c) Damage and vulnerability assessment of churches after the 2002 Molise, Italy, earthquake. Earthq Spectra 20(I):S271–S283. https://doi.org/10.1193/1.1767161

Lang K, Bachmann H (2004) On the seismic vulnerability of existing buildings: a case study of the city of Basel. Earthq Spectra 20(1):43–66. https://doi.org/10.1193/1.1648335

Marotta A, Sorrentino L, Liberatore D, Ingham JM (2016) Vulnerability assessment of unreinforced masonry churches following the 2010–2011 canterbury earthquake sequence. J Earthq Eng 21(6):912–934. https://doi.org/10.1080/13632469.2016.1206761

Milani G, Lourenco P (2011) CFE homogenised limit analysis model for masonry structures. Eng Comput Mech 164(2):65–78. https://doi.org/10.1680/eacm.2011.164.2.65

Minister of Heritage and Cultural Activities, Circular n.26, Italian Code for protection of cultural heritage. "Linee Guida per la valutazione e la riduzione del rischio Sismico del patrimonio culturale con riferimento alle norme tecniche per le costruzioni". Prot 10953 of 02/12/2010 (updated to 2011)

Sandi H, Floricel I (1994) Analysis of seismic risk affecting the existing building stock. In: Proceedings of the 10th European conference on earthquake engineering, Vienna, vol 2, A. A. Balkema, Rotterdam, pp 1105–1110

Tashkov L, Krstevska L, Naumovski N, De Matteis G, Brando G (2010) Ambient vibration tests on three religious buildings in Goriano Sicoli damaged during the 2009 L'Aquila earthquake. In: COST ACTION C26: Urban Habitat Constructions under Catastrophic Events, Proceedings of the Final Conference, pp 433–438

Valente M, Milani G (2018) Damage survey, simplified assessment, and advanced seismic analyses of two masonry churches after the 2012 Emilia earthquake. Int J Arch Heritage. https://doi.org/10.1080/15583058.2018.1492646